BIOCHEMICAL PHARMACOLOGY 73 (2007) 694–708

available at www.sciencedirect.com

ScienceDirect

journal homepage: www.elsevier.com/locate/biochempharm

Toxic effects of cobalt in primary cultures of mouse astrocytes
Similarities with hypoxia and role of HIF-1α☆

Olga Karovic[a], *Ilaria Tonazzini*[a], *Nelson Rebola*[a], *Erik Edström*[b], *Cecilia Lövdahl*[a], *Bertil B. Fredholm*[a], *Elisabetta Daré*[a,*]

[a] *Department of Physiology and Pharmacology, Karolinska Institutet, S-171 77 Stockholm, Sweden*
[b] *Department of Neuroscience, Karolinska Institutet, S-171 77 Stockholm, Sweden*

ARTICLE INFO

Article history:
Received 1 August 2006
Accepted 10 November 2006

Keywords:
Hypoxia
Apoptosis
Mitochondrial damage
Reactive oxygen species
Cobalt
ATP

ABSTRACT

Cobalt is suspected to cause memory deficit in humans and was reported to induce neurotoxicity in animal models. We have studied the effects of cobalt in primary cultures of mouse astrocytes. $CoCl_2$ (0.2–0.8 mM) caused dose-dependent ATP depletion, apoptosis (cell shrinkage, phosphatidylserine externalization and chromatin rearrangements) and secondary necrosis. The mitochondria appeared to be a main target of cobalt toxicity, as shown by the loss of mitochondrial membrane potential ($\Delta\Psi_m$) and release from the mitochondria of apoptogenic factors, e.g. apoptosis inducing factor (AIF). Pre-treatment with bongkrekic acid reduced ATP depletion, implicating the involvement of the mitochondrial permeability transition (MPT) pore. Cobalt increased the generation of oxygen radicals, but antioxidants did not prevent toxicity. There was also an impaired response to ATP stimulation, evaluated as a lower raise in intracellular calcium. Similarly to hypoxia and dymethyloxallyl glycine (DMOG), cobalt triggered stabilization of the α-subunit of hypoxia-inducible factor HIF-1 (HIF-1α). This early event was followed by an increased expression of HIF-1 regulated genes, e.g. stress protein HO-1, pro-apoptotic factor Nip3 and iNOS. Although all of the three stimuli activated the HIF-1α pathway and decreased ATP levels, the downstream effects were different. DMOG only inhibited cell proliferation, whereas the other two conditions caused cell death by apoptosis and necrosis. This points to cobalt and hypoxia not only inducing HIF-1α regulated genes but also affecting similarly other cellular functions, including metabolism.

1. Introduction

Cobalt is an essential element for humans since it is a necessary constituent for the formation of vitamin B12 (hydroxycobalamin). The human body contains about 1–2 mg of cobalt; most of it is found in the liver, kidney, heart and spleen, whereas low concentrations are detected in serum, brain and pancreas [1]. The minimum recommended

☆ This work was supported by Karolinska Institutet, the Swedish Science Research Council (2553), European Commission (LSHM-CT-2005-518189), the Swedish Brain Foundation, the T. Nilson Foundation, the Swedish Society of Medicine, the Å. Wiberg Foundation and the General Maternity Hospital foundation. The funding agencies do not take any responsibility for the contents of the article.

* *Corresponding author at:* Karolinska Institutet, Dept. of Physiology and Pharmacology, Section of Molecular Pharmacology, Nanna Svartz väg 2, S-171 77 Stockholm, Sweden. Tel.: +46 8 524 87933; fax: +46 8 34 12 80.
E-mail address: Elisabetta.Dare@ki.se (E. Daré).

0006-2952/$ – see front matter
doi:10.1016/j.bcp.2006.11.008

daily intake of hydroxycobalamin of an adult is 3 μg, corresponding to 0.012 μg of cobalt. Dietary vitamin B12 deficiency is a cause of anemia and increases the risk of developmental abnormalities and growth failure in infants [2]. However, excessive levels of cobalt can be detrimental to the organism. The route of exposure is frequently dermal or via inhalation [3] and occurs mostly in industrial refining, in the production of alloys and in the tungsten carbide hard metal industry. In urban areas mean concentration of cobalt in air is small (about 1–2 ng Co/m^3) but in heavily industrialised cities concentrations up to 10 ng/m^3 have been reported with concentrations near industrial sources ranging up to 600 ng Co/m^3 [4]. In occupational setting levels can be as high as 1100 μg Co/m^3 [5]. Increased levels of cobalt were found in urine and blood of occupationally exposed workers. For example, Ichikawa et al. [6] have reported that cobalt concentration was 0.57–0.79 μg/dl in blood and 59–78 μg/dl in urine following exposure to 100 μg/m^3.

Cobalt toxicity includes cardiomyopathy [7], adverse pulmonary effects [8] and carcinogenicity [9]. This heavy metal is also suspected to cause neurotoxic effects, as indicated by the report of memory deficit among workers exposed to hard metal both as dust powder and in mist form [10]. Uptake of cobalt in the nasal mucosa and transport to the olfactory bulbs may be an important route of brain exposure [11]. Experiments performed in the rat have shown that cobalt can cause decreased exploratory behavior [12] and depletion of neurotransmitters [13]. Besides inhibiting synaptic transmission by presynaptic blockade of calcium channels, cobalt can also block postsynaptic responses induced by neurotransmitters in vitro [14].

The data available in the literature indicate that cobalt is cytotoxic to many cell types, including neural cells [15–17] and can induce cell death by apoptosis and necrosis [18]. Cobalt can cause DNA fragmentation [19–21], activation of caspases [22], increased production of reactive oxygen species (ROS) [16,19,23], augmented phosphorylation of mitogen activated protein (MAP) kinases [17,22] and elevated levels of p53 [23].

Cobalt has been used to induce ischemic pre-conditioning in vivo [24]. Some of the characteristic effects of cobalt are thought to be mediated by interaction with the cellular oxygen-sensing machinery. Like low oxygen tension, cobalt at normoxic conditions is able to stabilize the α-subunit of hypoxia-inducible factor HIF-1 by blocking its ubiquitination and proteasomal degradation [25]. Increased levels of HIF-1α result in higher transcription of a set of genes that encode several proteins, e.g. glycolytic enzymes, erythropoietin and heat shock proteins, important for the adaptation of cells to hypoxic stress [26,27]. Many of the gene products regulated by HIF-1α are involved in a physiological response to promote cell survival and recovery after hypoxia, e.g. by maintenance of cellular energy supplies and stimulation of angiogenesis. However, recent work has also pointed to the increased transcription of pro-apoptotic factors, i.e. NIP3/BNIP3 and NIX [28], which can lead to cell death. Because of these effects cobalt ions may be used to elucidate the roles of HIF-1α in different types of cells.

Astrocytes play a crucial role in regulating functions and survival of neurons and controlling synapses [29,30]. Although glia are generally considered more resistant to stress conditions as compared to neuronal cells, recent studies have indicated that astrocytes are also susceptible to a variety of neurotoxic stimuli, including hypoxic injury and heavy metals [31–38]. It was reported that cobalt can activate extracellular signal-regulated protein kinase1/2 (ERK1/2) and cause cell death by apoptosis in C6 glioma cells [17], but otherwise little is known about cobalt effects in astrocytes. The purpose of the present study was twofold. First, we aimed to characterize cobalt cytotoxicity in primary astrocytes, by investigating the possible involvement of HIF-1 regulated genes, oxidative stress and calcium signaling, as well as by looking at mechanisms of cell death. On the other hand, we wanted to verify the hypothesis that cobalt is a valuable mimic of hypoxia in astrocytes. For this purpose, we have compared the effects of cobalt exposure to oxygen deprivation.

2. Materials and methods

2.1. Chemicals

All cell culture reagents, including media, antibiotics, fetal bovine serum (FBS) and phosphate buffered saline (PBS) were purchased from Gibco-Life Technologies (Täby, Sweden) and cell culture plastics from Corning Incorporated (Schipol-Rijk, NE). The RNeasy kit was obtained from Qiagen (VWR International, Stockholm, Sweden). The GeneAmp RNA PCR kit and the TaqMan Universal PCR master mix were purchased from Applied Biosystems (Applera Sweden, Stockholm). The fluorescein isothiocyanate (FITC)-annexin V, terminal transferase and fluorescein-12-UTP were purchased from Roche Diagnostics GmbH (Mannheim, Germany). The pan-caspase inhibitor Z-VAD-FMK was obtained from Enzyme Systems (Livermore, CA, USA) and dymethyloxallyl glycine (DMOG) was purchased from Cayman chemical (Ann Arbor, MI, USA). SB203580 was obtained from CalBiochem (Darmstadt, Germany). $CoCl_2$ (cell culture tested), *n*-propyl gallate (PG), *n*-acetyl-L-cysteine (NAC), n_ω-nitro-D-arginine methyl ester hydrochloride (L-NAME), L-N^6-(1-iminoethyl)lysine hydrochloride (L-NIL), 17β-estradiol, bongkrekic acid (BKA), cyclosporine A, 2-(2-amino-3-methoxyphenyl)-4H-1-benzopyran-4-one (PD98059), adenosine triphosphate (ATP), the lactate dehydrogenase (LDH) detection kit and the rest of the chemicals were purchased from Sigma–Aldrich (St. Louis, MO, USA). Enhanced chemiluminescence detection (ECL) kit was from Amersham Biosciences (Little Chalfont, Buckinghamshire, UK). Carboxy-dichlorodihydrofluoresceine diacetate (carboxy-H_2DCFDA), tetramethylrhodamine (TMRE) and Fluo-3 were bought from Molecular Probes (Invitrogen, Basel, Switzerland).

2.2. Cell culture and exposure to chemicals

The study was performed in accordance with the NIH *Guide for the Care and Use of Laboratory Animals* and was approved by the Animal Ethics Committee of Northern Stockholm. Primary cultures of mouse astrocytes were prepared from newborn C57Bl6 mice sacrificed by decapitation. The brains were rapidly dissected out, cerebellum and olfactory bulb were removed and the meninges and blood vessels were carefully

stripped off at the stereomicroscope. The tissue was chopped and transferred to complete Dulbecco's modified Eagle medium (DMEM) (i.e. supplemented with 10% FBS, 50 units/ml penicillin and 50 μg/ml streptomycin-sulphate) and dissociated by pipetting in order to generate a cell suspension, which was filtered through a 70-μm pore size mesh cell strainer. Cells were seeded at a density of 28,000 cells/cm^2 in poly-L-lysine-coated bottles and maintained in complete DMEM at 37 °C in a humidified atmosphere with 5% CO_2. The culture medium was changed on day in vitro (DIV)1, DIV5 and DIV7. On DIV9 the microglia were dislodged from the astrocyte cultures by shaking and they were discarded. The astrocytes were harvested from the flask with trypsin and reseeded at a density of 28,000 cells/cm^2. On DIV12 the cells were exposed to the various chemicals in F-12 medium supplemented with 10% FBS. Purity of the cultures was monitored by immunocytochemical detection of the astrocyte marker glial fibrillary acidic protein (GFAP) and neuronal marker β-III tubulin, as well as by identifying microglial cells with FITC-conjugated isolectin B4 (Sigma–Aldrich, 4 μg/ml).

2.3. Exposure to hypoxic environment

On DIV9 astrocytes were plated in 6- and 96-well plates. On DIV12 the medium was changed to F-12 supplemented with 10% FBS and the cultures were transferred to a CO_2 incubator (Queue, LABEQUIP™, Ontario, Canada) connected to a nitrogen source to obtain hypoxic conditions (1% O_2, 5% CO_2, 94% N_2). The measurements of O_2 concentration inside the incubator were performed with the Draeger Pac III analyzer (Draeger Safety mc., Pittsburg, PA, USA).

2.4. Luminescence ATP detection assay system

Astrocytes were plated in 96-well plates on DIV9 and exposed to the chemicals on DIV12. Cells were exposed to $CoCl_2$ (0.2–0.8 mM) for different time periods (3–48 h). In some experiments astrocytes were pre-treated with various substances (antioxidants, caspase inhibitor, iNOS inhibitors, mitochondrial permeability transition pore inhibitors, MAP kinase inhibitors) for 1 h prior to cobalt exposure for 3–24 h. In parallel cells were kept under hypoxic conditions for 3–24 h or exposed to 0.1–1.5 mM DMOG for 24 h. At the end of the treatments, the total ATP level in each well was measured with the ATP Lite™ kit, which is based on the production of light caused by the reaction of ATP with added firefly luciferase and D-luciferin. The luminescence was measured with a Trilux Micro Beta luminescence counter (Wallac, Upplands Väsby, Sweden). Statistical analysis was performed by using one-way ANOVA followed by Tukey's post hoc test.

2.5. Trypan blue exclusion test

On DIV12 astrocytes were exposed to $CoCl_2$ (0.2–0.8 mM), DMOG (1–1.5 mM), 0.4 mM H_2O_2 or hypoxia for 3–24 h. Cells were harvested with trypsin and pooled together with cells floating in the culture medium. An aliquot of this cell suspension was mixed with an equal volume of 0.4% trypan blue in phosphate buffered saline (PBS). Cells were scored at the phase contrast microscope using a Neubauer improved counting chamber. Cells with damaged cell membrane (necrotic cells) stained blue, while cells that maintained plasma membrane integrity prevented the dye entry and remained unstained (healthy cells and apoptotic cells). Statistical analysis was performed using either one-way analysis of variance (ANOVA) followed by Tukey's post hoc or two-tailed paired Student's *t*-test in GraphPad Prism2 software (GraphPad, San Diego, CA).

2.6. LDH assay

The astrocytes were seeded in 96-well plates on DIV9 and they were exposed to $CoCl_2$ (0.2–0.8 mM) for 24 h on DIV12. At the end of treatment, the cell membrane integrity was evaluated as a function of the amount of cytoplasmic LDH released into the medium, using an assay based on reduction of NAD by the action of LDH. The reduced NAD (NADH) was utilized in the stoichiometric conversion of a tetrazolium dye into a color compound, which was measured spectrophotometrically. The amount of LDH released into the medium was normalized against the total cell number. Statistical analysis was performed by using one-way ANOVA followed by Tukey's post hoc test.

2.7. Analysis of chromatin condensation by propidium iodide staining

Cells were plated on poly-L-lysine-coated coverslips on DIV9 and exposed to chemicals on DIV12, as described in Section 2.4. At the end of the exposure, the medium was removed and the astrocytes were fixed in ice-cold methanol at −20 °C for 30 min. Nucleic acid staining was obtained by using 5 μg/ml propidium iodide (PI). Stained samples were analyzed at the fluorescence microscope (Zeiss, Germany). The apoptotic nuclei were identified by irregular shape, smaller size and bright intensely stained chromatin. Nine fields were counted for each condition. Statistical analysis was performed by using one-way ANOVA followed by Tukey's post hoc test.

2.8. Detection of DNA fragmentation by terminal deoxyribonucleotide transferase (TdT)-mediated dUTP nick end labeling (TUNEL) assay

Astrocytes were plated on coverslips coated with poly-L-lysine on DIV9 and exposed to 0.2–0.8 mM $CoCl_2$ for 24 h on DIV12. Cells were then fixed in ice-cold methanol at −20 °C for 30 min. After two washes with PBS, the cells were incubated with TUNEL reaction mixture (0.07% Triton X-100, 2.5 mM $CoCl_2$, 5 μM fluorescein-12-UTP, 5 U/μl terminal transferase, 0.2 mM potassiumcacodylate, 0.25 mg/ml BSA, 25 mM Tris–HCl pH 6.6) at 37 °C in a moisturized dark chamber for 60 min. The cells were rinsed with PBS and stained with PI (5 μg/ml) for 5 min at room temperature to visualize the chromatin. The coverslips were washed with PBS and mounted onto slides with Dako fluorescent mounting medium (DakoCytomation). The nuclei were counted (nine fields for each condition) and photographed using a Zeiss Axioscop 2 plus fluorescent microscope equipped with Axio Cam camera and at the Zeiss LSM510 confocal microscope (Zeiss, Germany). Statistical analysis was performed by using one-way ANOVA followed by Tukey's post hoc test.

2.9. Vital triple staining

Annexin V is a phospholipid-binding protein with high affinity for phosphatidylserine. On DIV12 cells grown on coverslips were exposed to 0.5 mM $CoCl_2$ for 6–24 h, then incubated with a solution of FITC-annexin V (0.5 μg/ml), cell impermeable PI (1 μg/ml) and cell permeable Hoechst 33358 (10 μg/ml) in 10 mM HEPES/NaOH pH 7.4, 140 mM NaCl, 5 mM $CaCl_2$. Replicate coverslips were examined at the Zeiss Axioscop 2 plus fluorescence microscope. Images were collected with the Axio Cam camera.

2.10. Bromodeoxyuridine/PI double staining

On DIV12 astocytes grown on coverslips were exposed to 1.5 mM DMOG for 6 h. BrdU (Sigma) was added to the cultures 45 min before collecting the cells (final concentration 50 μg/ml). Cells were washed with PBS and fixed with 100% ethanol at −20 °C for 20 min. The coverslips were rinsed with PBS and incubated with 4 N HCl at 37 °C for 30 min. Blocking was performed with 1% BSA, 0.3% Triton in PBS at room temperature for 30 min. The coverslips were incubated with a FITC-conjugated anti-BrdU antibody (Abcam Ltd., Cambridge, UK, dilution 1:10 in the blocking solution) at 4 °C overnight, washed with PBS and stained with PI as described in Section 2.7. Nuclei were examined at the fluorescent microscope to evaluate the percentage of the BrdU positive cells.

2.11. Sodium dodecyl sulfate-polyacrylamide gel electrophoresis (SDS-PAGE) and immunoblotting

On DIV9 astrocytes were plated on 6-well plates. On DIV 12 cells were exposed to 0.2–0.8 mM $CoCl_2$, 1.5 mM DMOG and hypoxia for different time periods (3–24 h). Cells were washed with PBS and briefly sonicated in lysis buffer (150 mM NaCl, 1% Triton X-100, 10 mM Tris–HCl pH 7.4 supplemented with 1 mM phenylmethylsulfonyl fluoride, 1 μg/ml leupeptine, 1 mM sodium orthophosphate and 1 mM NaF) [39]. The protein concentration was measured with the Micro BCA assay kit (Pierce, Rockford, IL, USA). Subcellular extracts were prepared using ProteoExtract-Subcellular Proteome Extraction kit (Calbiochem, EMD Biosciences Inc., Darmstadt, Germany) and the protein concentration was measured with the DC Protein Assay kit (Bio-Rad Laboratories AB, Sundbyberg, Sweden). Proteins (30 μg/lane) were separated by SDS-PAGE and transferred into nitrocellulose transfer membrane (Schleicher & Schuell BioScience, Dassel, Germany) according to methods previously described [40]. Equal loading was verified by staining the membranes with 0.1% Ponceau S in 5% acetic acid (Sigma). The membranes were incubated overnight with the following primary antibodies: mouse monoclonal anti-poly(ADP-ribose) polymerase (PARP) antibody (dilution 1: 5000, BIOMOL Research Laboratories, Plymouth Meeting, PA, USA); rabbit anti-inducible nitric oxide synthase (iNOS) antibody (dilution 1:5000, Sigma–Aldrich, St. Louis, USA); rabbit polyclonal anti-phospho-p44/42 MAP kinase (THR202/Tyr204) antibody (dilution 1:2000, Cell Signaling Technology, Philadelphia, PA, USA); rabbit polyclonal anti-P44/42 MAP kinase antibody (dilution 1:1000, Cell Signaling Technology); rabbit anti-phospho p38 MAP kinase (Thr180/Tyr182) antibody (dilution 1:1000, BioLabs, New England, USA); mouse monoclonal anti-HIF-1α antibody (dilution 1:400, Abcam Ltd.); goat polyclonal anti-apoptosis inducing factor (AIF) antibody (dilution 1:200, Santa Cruz Biotechnology Inc., Santa Cruz, California); goat polyclonal anti-NIP3 antibody (dilution 1:200, Santa Cruz Biotechnology) and polyclonal rabbit anti-HSP72 antibody (dilution 1:10,000, Stressgen, Nordic Biosite, Täby, Sweden). After 1 h incubation with the proper horseradish peroxidase conjugated secondary antibody (dilution 1:10,000, Pierce), the membranes were incubated with ECL reagents for chemiluminescence (Amersham, Little Chalfont, Bucks, UK) and exposed to X-ray autoradiography films (Fuji, Japan). Quantification was performed by densitometry using the MCID-M5 (4.0 Rev. 1.3) image software. Statistical analysis was done by using one-tailed paired Student's *t*-test.

2.12. Immunocytochemistry

Detection of protein expression by immunocytochemistry was performed according to a procedure previously described [41]. Briefly, astrocytes were grown on coverslips, exposed to 0.5 mM $CoCl_2$ for 16 and 24 h on DIV12, and fixed in ice-cold methanol at −20 °C for 30 min. The coverslips were incubated overnight with the following primary antibodies: anti-GFAP (dilution 1:200, DAKO Cytomation, Älvjö, Sweden), anti-βIII-tubulin (dilution 1:200, Nordic Biosite AB, Täby, Sweden), anti-heme-oxygenase-1 (HO-1) (dilution 1:2000, Stressgen, Victoria, BC, Canada), and anti-iNOS (dilution 1:200, Santa Cruz Biotechnology). Next, the samples were incubated with the proper fluorescence-conjugated secondary antibody for 1 h. The nuclei were visualized by PI staining (5 μg/ml) for 5 min. The coverslips were mounted onto slides with Dako fluorescent mounting medium and analyzed at the Zeiss Axioscop 2 plus fluorescent microscope equipped with Axio Cam camera and at the Zeiss LSM510 confocal microscope.

2.13. ROS measurements

Formation of oxygen radicals was detected with carboxy-H_2DCFDA. Following uptake, the carboxy-H_2DCFDA is converted by endogenous esterases to carboxy-H_2DCF, which upon exposure to oxidative species is oxidized to the fluorescent probe carboxy-DCF. This dye fluoresces on interaction with ROS, including H_2O_2 and hydroxyl radical, but it is relatively insensitive to superoxide anion [42]. On DIV12 astrocytes were treated with 5 mM NAC 1 h prior exposure to 0.5 mM $CoCl_2$ or 0.4 mM H_2O_2 for 6 h. At the end of the incubation period carboxy-H_2DCFDA was added to the culture medium (20 μM) and the 96-well plates were kept at 37 °C for 30 min. Next, the cells were washed twice with a buffer containing 154 mM NaCl, 5.6 mM KCl, 5.6 mM glucose, 1 mM $MgCl_2$, 2.3 mM $CaCl_2$ and 8.6 mM HEPES pH 7.4. Carboxy-DCF fluorescence was measured in a Molecular Devices fluorescence counter (Spectramax GEMINI, Göteborgs Termometerfabrik, Sweden) using 485 nm excitation and emission 535 nm.

2.14. HIF-1α detection by ELISA

Astrocytes were seeded in 6-well plates on DIV9 and exposed to 0.5 mM $CoCl_2$ for 3 h on DIV12. A commercial ELISA kit (R&D

systems, Minneapolis, MN) was used to determine HIF-1α levels. The experiments were carried out according to manufacturer's protocol. Briefly, cells were rinsed twice with PBS and solubilized in lysis buffer. Lysates were vortexed, transferred to 96-well plates pre-coated with the Capture Antibody (mouse anti-human HIF-1α antibody) and incubated for 2 h. The wells were washed and incubated with the detection antibody (biotinylated goat anti-human HIF-1α antibody). Next, streptavidin conjugated to horseradish peroxidase was added. A final washing step was followed by chromogen reaction obtained by adding tetramethylbenzidine and H_2O_2 and stopped with H_2SO_4. The absorption of the samples at 450 nm was measured in a microplate reader (Labsysytems, Breda, The Netherlands), with 570 nm correction.

2.15. RNA extraction and cDNA synthesis

On DIV12 astrocytes were treated with 0.5 mM $CoCl_2$ for 0.5–24 h. RNA was isolated from cells using the reagents and protocols included in the Qiagen RNeasy kit. Astrocytes were homogenized in Qiagen lysis buffer using a syringe and needle before RNA extraction with the Qiagen columns. RNA quantity and quality was determined spectrophotometrically at 260 and 280 nm with an Eppendorf Biophotometer (Eppendorf, Hamburg, Germany). The cDNA synthesis was performed with the GeneAmp RNA PCR kit using random hexamers and the MuLV reverse transcriptase.

2.16. Real-time reverse transcription polymerase chain reaction (RT-PCR)

The expression of Nip3 was evaluated by semi-quantitative real-time PCR [43]. β-Actin primers and probe were obtained from MWG-Biotech AG (Ebersberg, Germany). The following sequences were used: primer 1, 5′-GCT CTG GCT CCT AGC ACC AT-3′; primer 2, 5′-CCA CCG ATC CAC ACA GAG TAC-3′; probe, 5′-ATC AAG ATC ATT GCT CCT CCT GAG CGC-3′ [44]. The TaqMan probe and primers for the gene expression assay of Nip3 were purchased as an Assay-On-Demand from Applied Biosystem (assay identity Mm00833810). The real time PCR reactions were performed in triplicates with the TaqMan Universal PCR master mix in an ABI Prism 7000 Sequence Detector System (Applied Biosystems). Values are expressed as the difference in the number of cycles to reach the detection threshold (Ct = cycle at threshold), using β-actin as reference ($\Delta Ct = Ct_{AR} - Ct_{\beta\text{-actin}}$).

2.17. Intracellular calcium $[Ca^{2+}]_i$ measurement

Changes in $[Ca^{2+}]_i$ induced by stimulation with ATP were evaluated using the fluorescent Ca^{2+}-sensitive dye Fluo-3. Astrocytes were plated on 96-well plates on DIV9. On DIV12 cells were exposed to 0.2–0.8 mM $CoCl_2$ for 2 min–24 h. Next, astrocytes were washed with prewarmed HEPES buffer (135 mM NaCl, 5 mM KCl, 1.8 mM $CaCl_2$, 0.62 mM $MgCl_2$, 6 mM glucose, 15 mM HEPES pH 7.4) and incubated with 7.3 μM Fluo-3 AM in HEPES buffer solution at 37 °C for 45 min. The plates were washed twice with HEPES buffer and placed in the Fluoroscan Ascent Spectrofluorimeter (Labsystems, Finland) set to 37 °C. Fluo-3 was excited at 488 nm and fluorescence emission was detected using a 535 nm band pass filter. Fluorescence was acquired every second using the user-customized program Ascent. After the background readings (F_0) (5 s) 20 μM ATP was added and the recording was continued for 20 s. The relative changes in $[Ca^{2+}]_i$ were determined by the fluorescence signal reading (F_t) with subtracted background ($\Delta F = F_t - F_0$).

2.18. Measurements of the mitochondrial membrane potential ($\Delta\Psi_m$)

Changes in $\Delta\Psi_m$ were detected using TMRE, which partitions to the negatively charged mitochondrial matrix according to the Nernst equation and acts as a voltage sensitive probe. TMRE fluorescence is reduced in parallel to decreases of $\Delta\Psi_m$ [45]. Cells were grown on coverslips and exposed to $CoCl_2$ (0.5 mM for 6 h) on DIV12. At the end of the exposure the medium was replaced with 25 nM TMRE in PBS and the cells were maintained at room temperature in the dark for 20 min, then cell permeable Hoechst (12 μM) was added and the incubation was continued for 10 min to counterstain the nuclei. The coverslips were mounted on slides and analysed immediately at the Zeiss Axioscop 2 plus fluorescence microscope, collecting images with the Axio Cam camera.

3. Results

3.1. Features of cobalt toxicity

Primary mouse astrocytes exposed to 0.2–0.8 mM $CoCl_2$ displayed both biochemical and morphological signs of cellular toxicity. These levels of cobalt are several orders of magnitude higher than plasma levels encountered in human exposure but similar to the doses used in previous experiments to affect metabolism. All of the doses tested induced a significant decrease of the total ATP level after 24 h (Fig. 1A). Depletion of ATP can be a consequence of metabolic alterations resulting in deficient ATP synthesis. Alternatively, an ATP decrease can reflect a change in cell number due to cell death or cell cycle arrest. In our cultures there was a decrease in ATP at 24 h after 0.5 and 0.8 mM $CoCl_2$ that could be partially accounted for by a decreased number of cells (Fig. 1B), although the differences were still significant after normalizing the ATP values with the total cell number (0.2 mM $CoCl_2$, 75.1%; 0.5 mM $CoCl_2$, 60.1%; 0.8 mM $CoCl_2$, 38.6%). The fact that at the 0.2 mM dose there was ATP depletion without cell death or inhibition of cell proliferation supported an effect of cobalt on ATP metabolism (Fig. 1). The first time point when we observed ATP depletion was at 6 h (control, 100 ± 6.05; 0.5 mM $CoCl_2$, 65.07 ± 6.40, $n = 5$, $^{**}p \leq 0.01$, Student's *t*-test) without any significant occurrence of necrosis, as assessed by trypan blue counting (data not shown). These data point to an effect of cobalt on ATP production.

Astrocytes exposed to ≥0.5 mM $CoCl_2$ also displayed typical features of cell death by apoptosis, e.g. the cells appeared shrunken as compared to control cells and nuclear staining revealed the presence of chromatin condensation (Figs. 2A and 3A). Several of the apoptotic nuclei showed DNA fragmenta-

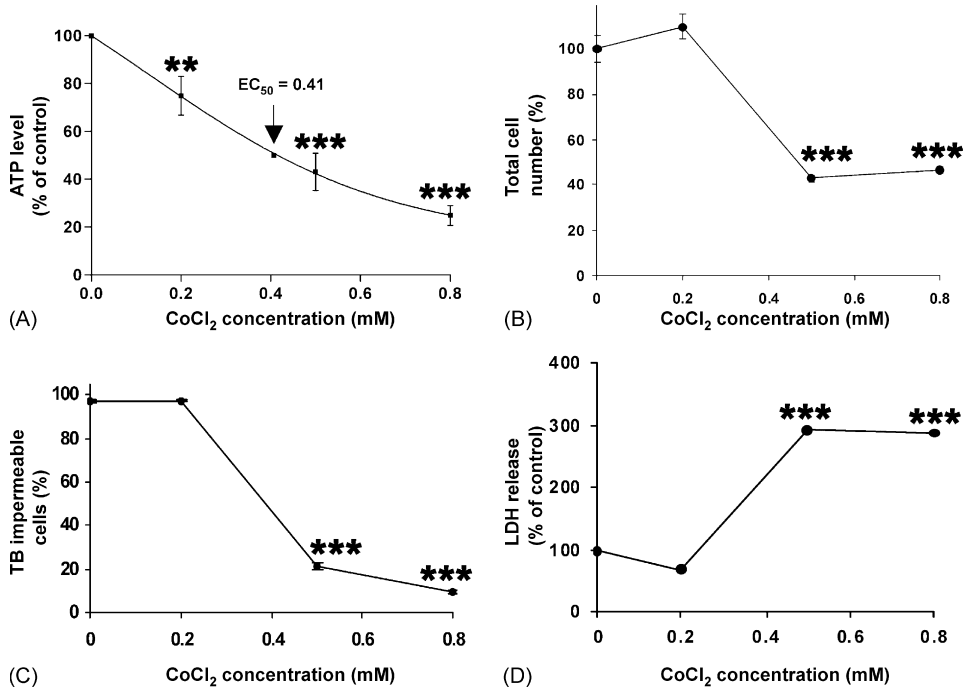

Fig. 1 – Cytotoxic effects detected in primary astrocytes exposed to 0.2–0.8 mM $CoCl_2$ for 24 h. Values are means ± S.E.M. $CoCl_2$ induced a dose-dependent ATP depletion (A) ($n = 7$ experiments) and reduction of the total cell number (B) ($n = 3$). Increase of the percentage of cells with alteration of the cell membrane permeability barrier was detected with the trypan blue (TB) test (C) ($n = 3$) and with the LDH release assay (D) ($n = 6$). Statistical analysis was performed with one-way ANOVA followed by Tukey's post hoc test ($^{**}p \leq 0.01$; $^{***}p \leq 0.001$).

tion, as revealed by the TUNEL assay (Figs. 2C and 3G and H). Time course analysis of nuclear morphology demonstrated chromatin rearrangements at 6 h (Fig. 2B). In addition, astrocytes had begun to display translocation of phosphatidylserine (PS) from the inner to the outer leaflet of the plasma membrane after 6 h exposure, as shown by FITC-annexin V binding in cells excluding propidium iodide (Fig. 3I–L). The PS externalization increased in the following hours. Translocation of PS is a typical structural modification occurring during apoptosis allowing recognition of dead cells by phagocytes in the so called "resolution phase". Due to the lack of proper phagocytic activity in our culture model the cells progressed instead into "secondary necrosis". This was shown by the conspicuous loss of membrane integrity revealed by trypan blue uptake and increased leakage of the cytoplasmic enzymes LDH in the extracellular medium at the 0.5 and 0.8 mM doses after 24 h (Fig. 1C and D).

Since apoptotic pathways often converge in the activation of class II caspases [46] we studied their activation by analyzing the cleavage of the repair enzyme PARP (116 kDa), generating a characteristic 85 kDa fragment [32]. Exposure to $CoCl_2$ for 6–24 h was not associated with significant cleavage of PARP (Fig. 2D). Furthermore, pre-treatment of the cultures for 1 h with the pan-caspase inhibitor Z-VAD-FMK (20 μM) neither ameliorated the ATP decrease (Table 1) nor reduced chromatin condensation (Table 2). Thus, caspases are unlikely to play a major role in cobalt-induced apoptosis.

Cells exposed to 0.2 mM $CoCl_2$ for 24 h showed minor signs of cytotoxicity. In spite of the ATP depletion (Fig. 1A), there was no significant increase of the percentage of apoptotic nuclei (Fig. 2A and C) and no indication of necrosis (Fig. 1C and D). However, after 48 h the ATP level was further diminished as compared to control and the percentage of cells with condensed chromatin increased considerably (Table 3), indicating that at this dose of $CoCl_2$ apoptosis was simply delayed. Heavy metals are known to induce transcription of the Hsp72 gene that can protect the cells from stress. Increased levels of HSP72 protein have been shown to have protein repair functions and anti-apoptotic effects [47]. Western blot analysis of protein extracts revealed that HSP72 was greatly increased in astrocytes exposed to 0.2 mM $CoCl_2$ for 16 h (Fig. 2E). This could partially explain the higher cell survival at this concentration of $CoCl_2$ (Figs. 1 and 2A and C).

3.2. *Mitochondrial damage and AIF release*

We decided to focus on the 0.5 mM dose for a more thorough characterization of $CoCl_2$ effects, looking for the up-stream events responsible for the so-called "initiation phase" of the apoptotic process. The loss of ATP pointed to a possible involvement of mitochondrial damage in cobalt toxicity. We evaluated the mitochondrial membrane potential ($\Delta\Psi_m$) by using the voltage sensitive probe TMRE. Cobalt exposure for 6 h caused a loss of $\Delta\Psi_m$, as shown by lack of TMRE staining (Fig. 4B). In order to see if the alterations of the $\Delta\Psi_m$ were linked to the opening of the mitochondrial permeability transition (MPT) pore, we tested the effects of BKA, a MPT pore inhibitor. Pre-treatment with BKA significantly reduced

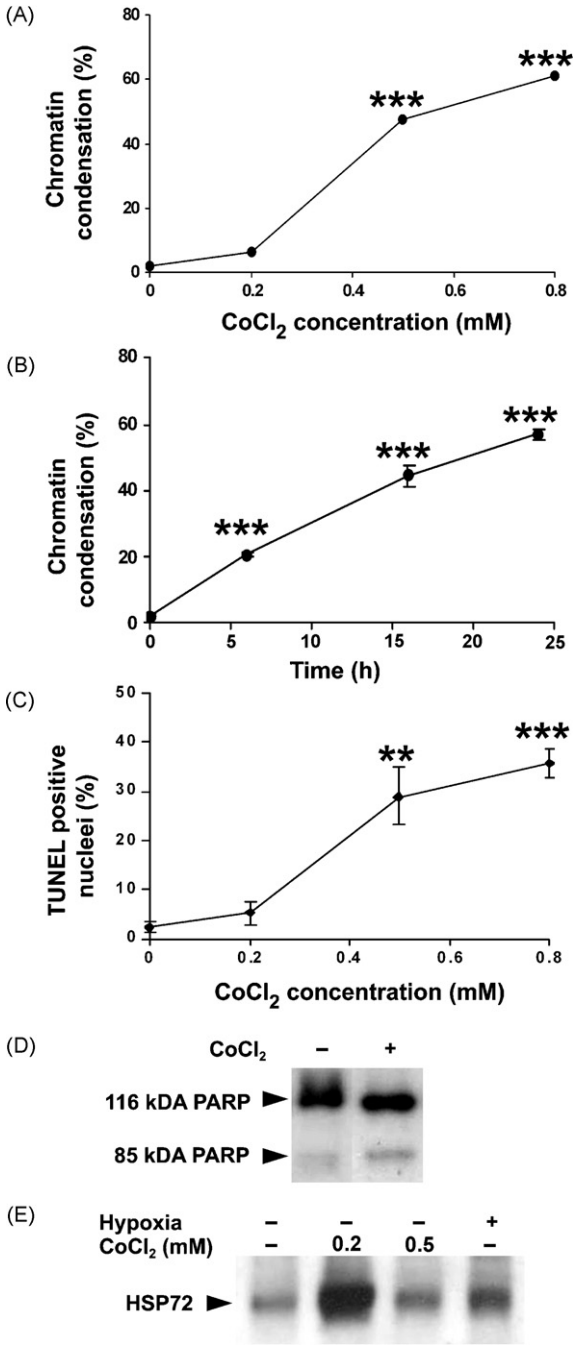

Fig. 2 – Analysis of apoptosis induced by $CoCl_2$. (A) The percentage of nuclei with chromatin condensation was determined by PI staining after exposure for 24 h to 0.2–0.8 mM $CoCl_2$. (B) Time course study of nuclear condensation following exposure to 0.5 mM $CoCl_2$. The increase in apoptotic nuclei was time dependent. (C) Evaluation of the percentage of nuclei with DNA fragmentation by TUNEL assay. Values in A–C are means ± S.E.M. Statistical analysis was performed with one-way ANOVA followed by Tukey's post hoc test ($^{**}p \leq 0.01$; $^{***}p \leq 0.001$, vs. control). (D) Analysis of PARP cleavage by immunoblotting in protein extracts obtained from astrocytes exposed to 0.5 mM $CoCl_2$ for 16 h and controls. The anti-PARP antibody detects both the intact form (116 kDa) and the 85 kDa-fragment generated by caspase degradation. (E) Western blot analysis of the expression of the stress protein HSP72 in astrocytes exposed to either $CoCl_2$ or hypoxia for 16 h.

the ATP depletion caused by cobalt after 6 h (control, 100 ± 6.05; 5 μM BKA, 108.61 ± 5.48; 0.5 mM $CoCl_2$, 65.07 ± 6.40; 0.5 mM $CoCl_2$ + 5 μM BKA, 91.6 ± 3.60, means ± S.E.M., $n = 5$, $^{*}p \leq 0.05$) as well as after 24 h (Table 1). A similar protection was observed after pre-treatment with the MPT pore inhibitor cyclosporine A (1 μM) (Table 1). These results imply that the MPT pore opening is one of the mechanisms contributing to the ATP decrease. Nevertheless, the protection by BKA was only partial because the percentage of apoptotic nuclei at 24 h was unchanged (Table 2). Apoptogenic mitochondrial factors are usually released as a consequence of the MPT pore opening or other damage of the mitochondrial membrane. Analysis of subcellular fractions by Western blotting revealed that cobalt caused the translocation of AIF from the mitochondria to the cytosol (Fig. 4E). This could explain the formation of apoptotic chromatin even in the absence of caspase activation because AIF is sufficient to induce chromatin condensation and DNA cleavage. The data point to a critical role of mitochondrial alterations in apoptosis induced by cobalt.

3.3. *ROS formation and effects of antioxidants*

Previous work has suggested that oxidative stress may be involved in the process of cell death induced by cobalt [16,19,48]. In order to test the hypothesis that excessive formation of ROS may substantially contribute to the toxic effects of cobalt also in astrocytes, we measured oxygen radicals using the carboxy-H_2DCFDA dye. Exposure to $CoCl_2$ for 6 h induced a modest but significant increase in ROS, which was abolished by pre-treatment with the antioxidant *n*-acetyl-L-cysteine (5 mM) (Fig. 5), a glutathione precursor as well as H_2O_2 and hydroxyl radical scavenger [49,50]. However, neither *n*-acetyl-L-cysteine nor other compounds with antioxidant properties, such as the general radical scavenger *n*-propyl-gallate (50 μM) [51] and the peroxy radical scavenger 17β-estradiol (20 μM) [52], could ameliorate the ATP decrease caused by $CoCl_2$ (Table 1). In addition, *n*-propyl-gallate did not prevent chromatin condensation (Table 2), although it was efficient in reducing apoptosis caused by 0.4 mM H_2O_2 (data not shown). Altogether these results indicate that oxidative stress does not have a critical role in triggering $CoCl_2$ toxicity in primary astrocytes.

3.4. *Activation of the HIF-1α pathway by hypoxia, $CoCl_2$ and DMOG*

Both the lack of oxygen and cobalt are known to stabilize the α-subunit of the transcription factor HIF-1 via inhibition of its degradation. We found a higher level of HIF-1α after 3 h of oxygen deprivation in our astrocyte cultures (Fig. 6A). This was followed by increased expression of HIF-1 regulated genes, such as HO-1 (Fig. 6B). Astrocytes exposed to hypoxia showed ATP depletion (control, 100 ± 2.52; 24 h hypoxia, 93.73 ± 2.04, $n = 7$, $^{*}p \leq 0.05$ Student's *t*-test) and displayed signs of apoptosis, e.g. chromatin condensation (Fig. 6C). A significant

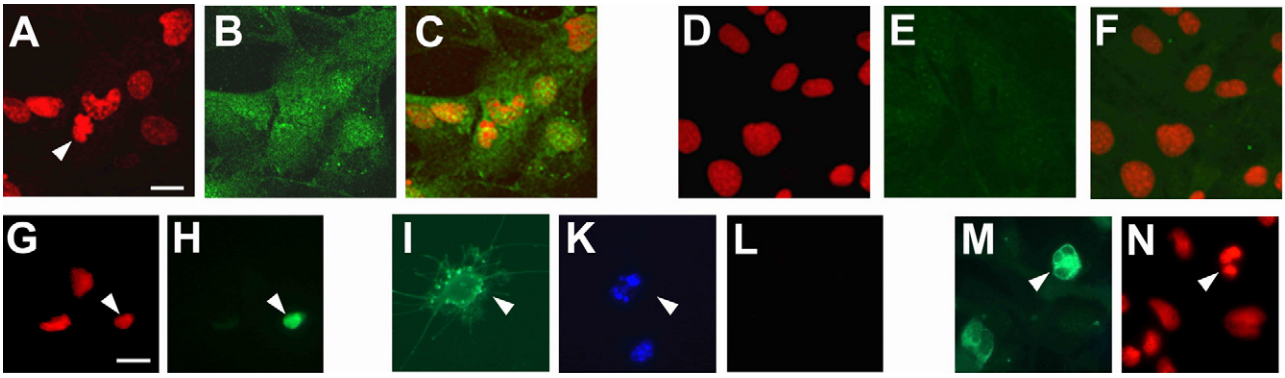

Fig. 3 – (A–F) Double staining of astrocytes with PI to visualize the chromatin (A, D red color) and with an anti iNOS antibody (B, E green color). Astrocytes exposed 0.5 mM $CoCl_2$ for 24 h (A–C) displayed apoptotic nuclei (see arrowhead in A) and increased expression of iNOS (B) as compared to control cells (D–F). Pictures were collected at the confocal microscope (C, merging of A and B; F, merging of D and E). (G–H) detection of chromatin fragmentation with the TUNEL assay in astrocytes exposed to 0.5 mM $CoCl_2$ for 24 h. Nuclei with DNA breaks are labeled in green (H), whereas the chromatin, visualized by PI staining, appears red (G). Note that in this field there are three apoptotic nuclei but only one, indicated by the arrow, is TUNEL positive. (I–L) Detection of PS externalization by annexin V staining. At the end of the incubation with $CoCl_2$ for 6 h, cells were immediately triple stained with cell membrane permeable Hoechst (K), annexin V (I) and cell membrane impermeable PI (L). Arrowheads indicate cells with condensed chromatin (K) displaying also annexin V positivity (I), without being permeable to PI (L). (M–N) Immunocytochemical detection of the expression of HO-1 in astrocytes exposed to 0.5 mM $CoCl_2$ for 24 h. HO-1 expression (M) was pronounced in cells with condensed chromatin (N), as pointed by the arrowhead. (For interpretation of the references to color in this figure legend, the reader is referred to the web version of the article.)

increase of necrosis was observed after hypoxia for 24 h (percentage of trypan blue impermeable cells: control, 100 ± 4.48, hypoxia, 86.04 ± 2.04, $n = 3$, $^{*}p \leq 0.05$ Student's *t*-test) but not at earlier time points.

Exposure to 0.5 mM $CoCl_2$ for 3 h stabilized HIF-1α as well, as shown by both Western blotting and ELISA (Figs. 6A and 7A), and there was a higher expression of HO-1 starting from 6 h (Figs. 3M and 6B). We looked at the expression of other HIF-1 regulated genes that could participate in cobalt toxicity such as Nip3 and iNOS. Nip3 encodes a pro-apoptotic factor belonging to the Bcl-2 family, which has been reported to cause cell damage by translocation to the mitochondrial membranes [53,54]. Using semi-quantitative real-time RT-PCR we found increased expression of Nip3-mRNA in cobalt-exposed cells (Fig. 7B). In agreement, a higher level of NIP3 protein was found after cobalt exposure (Fig. 7C), as well as following hypoxia (Fig. 6D).

HIF-1 is known to up-regulate the expression of inducible nitric oxide synthase (iNOS), able to cause detrimental effects via increased production of nitric oxide (NO) [27]. We found that the expression of iNOS was elevated in astrocytes exposed to $CoCl_2$ for 16 h by immunocytochemisty (Fig. 3B) and Western blotting (Fig. 7D). However, pre-incubation with selective iNOS inhibitors L-NAME and L-NIL could not protect the cells from either ATP depletion or chromatin condensation (see Supplemental material, Table S1 and S2).

To see if the activation of the HIF-1α pathway could be the cause of apoptosis, we exposed the astrocytes to DMOG, a well-known inhibitor of the prolyl hydroxylases responsible for the ubiquitination and proteasomal degradation of HIF-1α. As a consequence of HIF-1α stabilization (Fig. 6A), DMOG increases the expression of HIF-1 regulated genes, i.e. HO-1 (Fig. 6B). Astrocytes were exposed to DMOG (0.1–1.5 mM) in order to investigate ATP levels. Only doses ≥1 mM caused significant ATP depletion (not shown). Although 1.5 mM DMOG caused a decrease in ATP similar to that induced by 0.5 mM $CoCl_2$ (Table 4 and Fig. 1A), in this case no significant apoptosis was found (Table 4). Analysis of chromatin condensation at later time

Table 1 – Effects of pre-incubation with various compounds on ATP levels

	Control	Pre-treatment	0.5 mM $CoCl_2$	Pre-treatment + 0.5 mM $CoCl_2$
Z-VAD-FMK (20 μM) (caspase inhibitor)	100 ± 3.06	110.7 ± 2.10	40.9 ± 1.34	35.7 ± 1.06
n-Propyl gallate (50 μM) (antioxidant)	100 ± 3.06	84.1 ± 2.59	40.9 ± 1.34	$27.7 \pm 1.47^{**}$
17β-Estradiol (20 μM) (antioxidant)	100 ± 3.06	89.1 ± 2.91	40.9 ± 1.34	36.3 ± 1.19
n-Acetyl-L-cysteine (5 mM) (antioxidant)	100 ± 3.53	104.0 ± 5.67	21.2 ± 1.20	23.9 ± 1.53
Bongkrekic acid (5 μM) (MPT pore inhibitor)	100 ± 1.34	120.2 ± 5.11	34.5 ± 2.17	$60.7 \pm 3.42^{***}$
Cyclosporin A (1 μM) (MPT pore inhibitor)	100 ± 2.15	123.4 ± 1.43	20.8 ± 1.43	$37.9 \pm 1.79^{***}$

Astrocytes were pre-treated 1 h prior to addition of 0.5 mM $CoCl_2$ for 24 h. The experiments reported in the table were performed with different batches of cells. Values (means ± S.E.M., $n = 6$–8) are expressed as percentage of control. Statistical analysis was performed with one-way ANOVA followed by Tukey's post hoc test ($^{**}p < 0.01$; $^{***}p < 0.001$).

Table 2 – Analysis of chromatin condensation in astrocytes pre-incubated for 1 h with various compounds prior exposure to 0.5 mM $CoCl_2$

	Control	Pre-treatment	0.5 mM $CoCl_2$	Pre-treatment + 0.5 mM $CoCl_2$
Z-VAD-FMK (20 μM) (caspase inhibitor)	2.4 ± 0.70	4.9 ± 1.22	34.5 ± 2.58	30.1 ± 2.25
n-Propyl gallate (50 μM) (antioxidant)	2.1 ± 0.29	3.7 ± 0.33	56.9 ± 1.58	74.5 ± 1.22***
Bongkrekic acid (5 μM) (MPT pore inhibitor)	1.9 ± 1.94	2.7 ± 0.91	47.6 ± 2.06	45.9 ± 1.81

Values (means ± S.E.M., $n = 9$) are expressed as percentage of nuclei with condensed chromatin. Statistical analysis was performed with one-way ANOVA followed by Tukey's post hoc test (***$p < 0.001$ vs. 0.5 mM $CoCl_2$). The experiments reported in the table were performed with different batches of cells.

points (36 h) confirmed that DMOG (1 mM) did not cause apoptotic cell death (percentage of chromatin condensation: control, 3.28 ± 1.02; DMOG, 5.66 ± 1.46). DMOG instead inhibited cell proliferation, as measured by Brdu incorporation (Table 4). This reduction of cell number could explain the lower ATP levels measured in the cultures. We concluded that HIF-1α stabilization per se was not sufficient to induce apoptotic cell death in primary astrocytes.

3.5. *Alterations of calcium signaling*

Prolonged increases of intracellular calcium can contribute to cell death, for example via swelling and uncoupling of the mitochondria and by activation of proteases. We measured $[Ca^{2+}]_i$ with the calcium sensitive dye Fluo-3. Basal levels of $[Ca^{2+}]_i$ were unchanged after exposure to cobalt as compared to control, both at early time points (Fig. 8) and after 24 h (not shown). Stimulation of P2 receptors with 20 μM ATP caused the expected $[Ca^{2+}]_i$ increase in control cells (Fig. 8). In contrast, exposed astrocytes displayed an altered response to ATP. At 0.5–0.8 mM $CoCl_2$ the $[Ca^{2+}]_i$ rise was reduced after 1 h (Fig. 8A) and abolished after 3 h (Fig. 8B). Astrocytes exposed to the 0.2 mM dose had a reduced $[Ca^{2+}]_i$ increase after 3 h (Fig. 8B) and they did not respond at all to ATP after 16 h exposure (not shown). These results suggest that the disruption of calcium signaling is one of the relevant mechanisms of cobalt toxicity in astrocytes.

4. Discussion

Exposure to cobalt induced multiple alterations in primary astrocytes. Early events included stabilization of HIF-1α, resulting in increased expression of HIF-1 regulated genes, e.g. stress protein HO-1, pro-apoptotic factor NIP3 and iNOS. There was also altered calcium signaling and increased generation of oxygen radicals. Mitochondria were a key target of cobalt toxicity, as shown by loss of $\Delta\Psi_m$, opening of the MPT pore and release of AIF. This led to apoptosis, i.e. cell shrinkage, PS flip-flop and chromatin rearrangements, followed by secondary necrosis.

Table 3 – Exposure to 0.2 mM $CoCl_2$ for 48 h induced ATP depletion and increased the number of nuclei displaying chromatin condensation

Treatment (48 h)	ATP level (% of control) ($n = 4$)	Chromatin condensation (%) ($n = 9$)
Control	100 ± 2.72	1.9 ± 0.24
0.2 mM $CoCl_2$	43.1 ± 4.39****	61.8 ± 5.27****

Values are means ± S.E.M. (****$p \leq 0.0001$, significantly different from control, Student's *t*-test).

At the lowest dose of cobalt tested (0.2 mM) cytotoxicity was markedly delayed. This could be due to an initial activation of a stress response, as indicated by a pronounced expression of HSP72 and HO-1 (Karovic et al., unpublished) after 16 h, which can allow cells to adapt to the toxic environment. Transcription of the Hsp72 gene can be induced by a variety of heavy metals, including cobalt [55]. The activity of HSP72, which involves salvaging of denaturated proteins or chaperoning them to degradative system, has the potential to counteract the effects of cobalt, which has known ability to bind tightly and irreversibly to proteins [56]. In addition, HSP72 has been reported to reduce apoptosis via inhibition of stress-kinase JNK [47]. HO-1 also exerts protective functions, by controlling the redox state of the cell [57]. HO are rate limiting enzymes in the heme degradation. This process produces biliverdin, which is converted into bilirubin, free iron and carbon monoxide. Both biliverdin and bilirubin are potent antioxidants.

Cobalt caused dose-dependent ATP depletion. The ATP decrease was an early event and could not be modulated by antioxidants or by a broad caspase inhibitor. The ATP depletion could not be simply explained as decreased number of cells or necrosis, pointing to a disturbance in ATP production. Notably, cobalt has been reported to interfere with the Krebs cycle, causing inhibition of mitochondrial respiration of citrate and α-ketoglutarate [58]. Depletion of ATP has earlier been shown to follow exposure to cobalt in rat myocardium [59]. In this tissue the mechanism may be linked to a reduced manganese-superoxide dismutase (Mn-SOD) activity [59,60]. In our setting the lowering of ATP was less pronounced in cells pre-treated with BKA and cyclosporine A, suggesting that it was partly related to mitochondrial damage. Mitochondria were an early target of cobalt toxicity in astrocytes, as shown by the loss of $\Delta\Psi_m$ after 6 h. The collapse of the mitochondria involved the opening of the MPT pore and the release of apoptogenic factors, such as AIF. The mitochondrial proteins AIF and Endonuclease G can translocate to the nucleus and induce apoptotic changes in the chromatin independently from caspase activation [46,61].

Another factor pointing to alterations of the mitochondria by cobalt in astrocytes was the increased generation of oxygen radicals. Cobalt was reported to cause accumulation of H_2O_2 in granulosa and Hep3B cells and to induce production of hydroperoxyl radical and superoxide in a rat liver microsomal

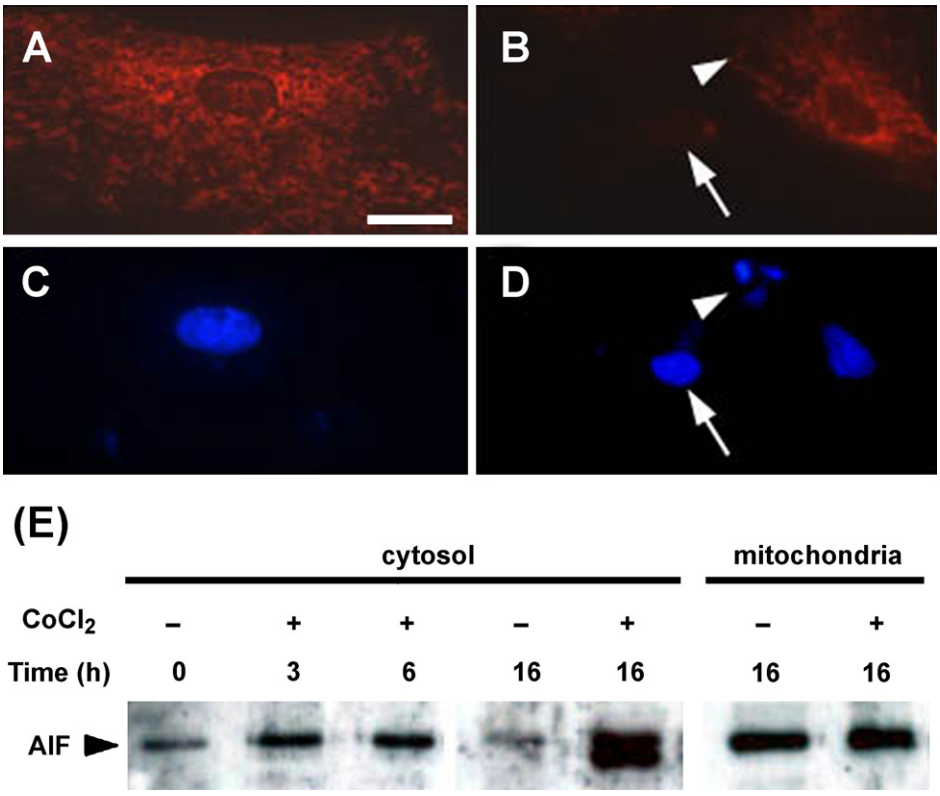

Fig. 4 – Mitochondrial damage caused by $CoCl_2$. The mitochondrial membrane potential was evaluated with the voltage-sensitive fluorescent dye TMRE (A and B), whereas the nuclei were visualized by Hoechst staining (C and D). Astrocytes exposed to $CoCl_2$ (0.5 mM) for 6 h showed a decrease in TMRE fluorescence (arrow and arrowhead in B) as compared to control cells (A), suggesting loss of $\Delta\Psi_m$. At the same time they displayed chromatin rearrangements, such as nuclear condensation and fragmentation (arrow and arrowhead, respectively, in D) as compared to control cells (C). (E) Analysis of AIF translocation from the mitochondria to the cytosol by immunoblotting, using subcellular fractions obtained from astrocytes exposed to 0.5 mM $CoCl_2$ for 3–16 h.

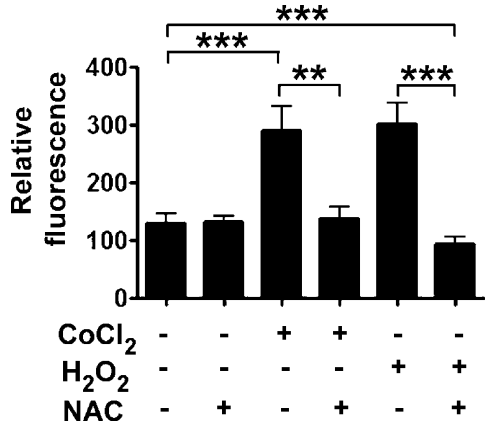

Fig. 5 – Exposure to either $CoCl_2$ (0.5 mM) or H_2O_2 (0.4 mM) for 6 h increased ROS formation in primary astrocytes. These effects were abolished by pre-incubation with NAC (5 mM) for 1 h. Oxygen radicals were measured with carboxy-H_2DCFDA. Values are means ± S.E.M., $n = 6$. Statistical analysis was performed by one-way ANOVA followed by Tukey's post hoc test ($^{**}p < 0.01$; $^{***}p < 0.001$).

system [62–64]. Moreover, cobalt was found to cause glutathione depletion in neuroblastoma SHSY5Y cells and rat liver [16,65], as well as ROS accumulation via a process not requiring mitochondrial electron transport in MCF-7 cells [23]. Oxidative stress-mediated activation of the nuclear transcription factor AP-1 and protection from apoptosis by antioxidants were described in cobalt-exposed PC12 cells [19]. In our glial cultures the ROS increase was rather small, perhaps due to the concomitant increased expression of HO-1, which can prevent generation of oxygen radicals [57]. Moreover, antioxidants did not protect from chromatin condensation or ATP loss. The same was also true for human alveolar macrophages [20] and mouse embryonic fibroblasts [53], showing that mechanisms by which cobalt chloride induces cellular damage and death may differ markedly between cell types. Although our data suggest that important aspects of cobalt cytotoxicity are independent of oxidative stress in astrocytes, it is possible that the small change in the redox state contributes to the induction of the HIF-1α pathway, as shown in other studies [66].

An increase in cytosolic Ca^{2+} is a common feature of many forms of cell death, and can potentiate the generation of ROS [67]. Aley et al. [68] have recently shown that hypoxia mobilizes Ca^{2+} from intracellular stores. We did not detect changes in the basal level of $[Ca^{2+}]_i$ following cobalt exposure,

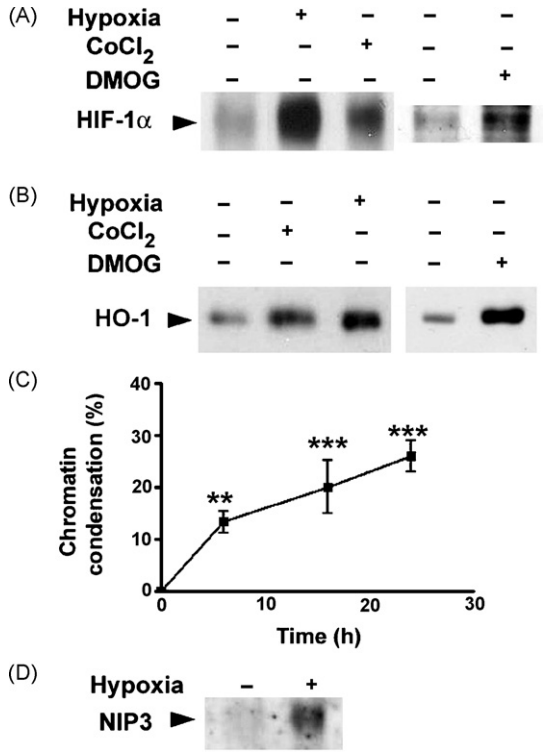

Fig. 6 – Alterations induced by hypoxia and $CoCl_2$. (A) Western blot detection of HIF-1α in astrocytes exposed to hypoxia, $CoCl_2$ (0.5 mM) or DMOG (1.5 mM) for 3 h. (B) Increased expression of HO-1 was found after the treatment with either 0.5 mM $CoCl_2$ or hypoxia for 6 h, as well as after exposure to DMOG (1.5 mM for 16 h). Hypoxic conditions caused a significant increase in chromatin condensation ($^{**}p \leq 0.01$; $^{***}p \leq 0.001$, vs. control), as detected by PI staining (C), and a higher expression of NIP3 after 6 h, as evaluated by Western blotting (D).

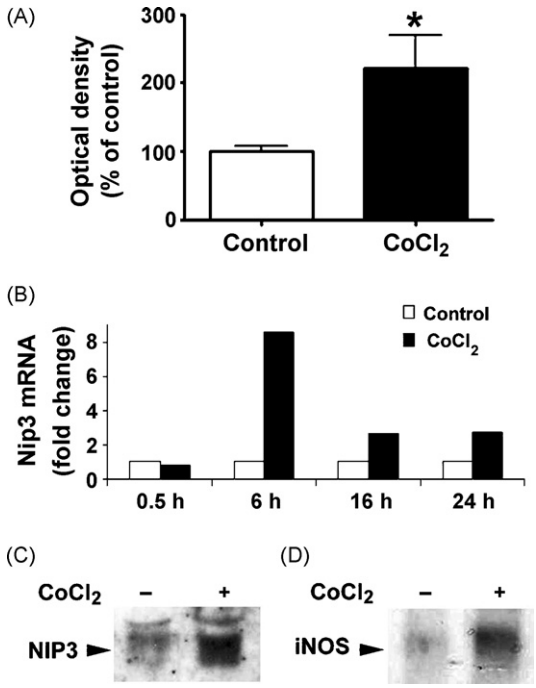

Fig. 7 – Activation of the HIF-1α pathway by 0.5 mM $CoCl_2$. (A) Increased expression of HIF-1α was found by ELISA in primary astrocytes exposed to $CoCl_2$ for 3 h (control, 101.1 ± 7.39; 0.5 mM $CoCl_2$, 220.9 ± 48.36, $n = 5$, $^{*}p \leq 0.05$ Student's *t*-test). (B) Semi quantitative RT-PCR revealed an increased expression of Nip3 mRNA after 6–24 h and immunoblots showed a higher level of the NIP3 factor after 6 h (C). The expression of iNOS was increased after 16 h, as shown by Western blotting (D).

even at late time points when there was collapse of the mitochondria. This may relate to the blockade of voltage activated calcium channels by cobalt [69], resulting in reduced calcium influx and, perhaps, depletion of intracellular calcium stores, e.g. mitochondria and endoplasmic reticulum. We did not study this directly but found that $[Ca^{2+}]_i$ increase induced by ATP was dose-dependently reduced, indicating effects on many types of Ca^{2+} channels.

Cobalt is commonly used as a mimic of hypoxia and as a stimulus to induce pre-conditioning in experimental models [24]. We attempted a comparison among cobalt exposure, oxygen deprivation and treatment with DMOG in primary astrocytes. Our data show that these three stimuli induced similarly the expression of HIF-1 regulated genes, confirming the gene expression profile recently obtained from oxygen-deprived rat astrocytes [70]. The levels of HIF-1α have been found increased also during brain ischemia in the rat [24,71] and associated with markers of apoptosis after traumatic brain injury [72]. In our glial cell model HIF-1α stabilization elevated the level of proteins that can potentially contribute to cell death, i.e. iNOS and NIP3. However, the activation of the HIF-1α pathway led to different effects depending on the stimulus used. The HIF-1α stabilizer DMOG caused ATP changes that mirrored inhibition of cell proliferation and did not lead to cell death. In contrast, both hypoxia and cobalt exposure were associated with compromised ATP production, possibly linked to metabolic changes, which resulted in death of the astrocytes. This is certainly due to additional cellular mechanisms modified by cobalt and hypoxia as compared to DMOG. We can conclude that HIF-1α stabilization is not sufficient to cause apoptosis in our model.

Table 4 – Cytotoxic effects due to stabilization of HIF-1 α by exposure to DMOG

End-point of cytotoxicity	Time (h)	Control	DMOG (1.5 mM)
ATP, $n = 4$	24	100 ± 2.78	58.23 ± 2.06***
Chromatin condensation (%) $n = 12$	24	5.27 ± 0.74	6.71 ± 1.15
Total cell number ($\times 10^3$), $n = 4$	16	352 ± 36	247 ± 27**
Brdu incorporation (%), $n = 16$	6	17.1 ± 3.20	8.4 ± 1.78*

Values are means ± S.E.M. Statistical analysis was performed with the Student's *t*-test ($^{*}p \leq 0.05$; $^{**}p \leq 0.01$; $^{***}p \leq 0.001$).

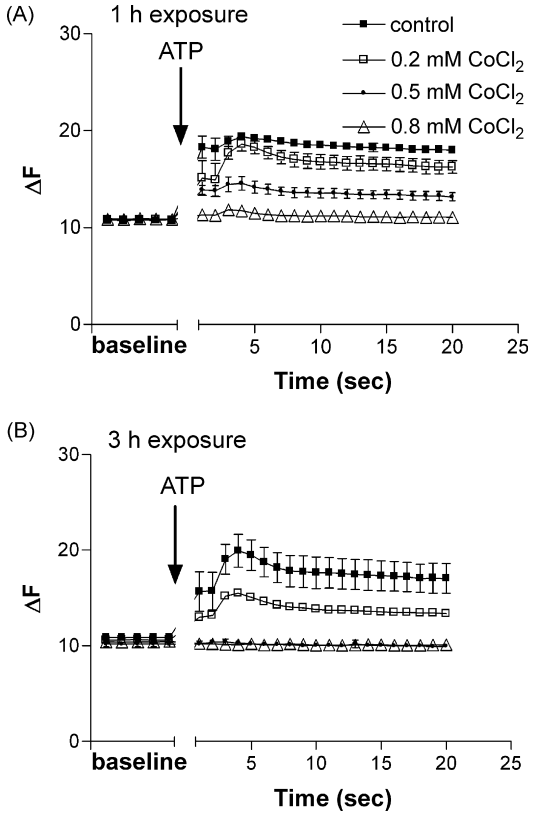

Fig. 8 – $CoCl_2$ reduced the response to ATP stimulation. $[Ca^{2+}]_i$ was measured with Fluo-3 in astrocyte cultures exposed to $CoCl_2$ either for 1 h (A) or 3 h (B). After baseline recording for 5 s, cells were stimulated with 20 μM ATP and the recording was continued for 20 s. Values (means ± S.E.M., $n = 3$) are expressed as $\Delta F = F_t - F_0$, i.e. the fluorescence signal reading at 535 nm (F_t) with background (F_0) subtracted.

Here we show that cobalt exposure recapitulates a number of events reported under hypoxic-ischemic conditions in astrocytes in vivo and in vitro, including PS externalization, DNA fragmentation and chromatin condensation, as well as mitochondrial damage and a modest increase in ROS generation [31,32,73]. Both cobalt exposure and oxygen deprivation caused ATP depletion in our astrocyte cultures, but ATP was decreased to a lower extent by hypoxia, suggesting that cobalt has additional distinct cellular targets.Gene expression profiling has shown that cobalt not only increases a battery of genes similar to that upregulated by hypoxia, but also regulates some specific genes, e.g. metallothionein 1 [74]. We and other have reported that it induces HSP72 [55]. Furthermore, cobalt is a well-known blocker of voltage-gated calcium channels, which may be the reason of its inhibition of morphological differentiation induced by cAMP in astrocytes [69,75]. We have found inhibition of calcium signaling, measured as response to ATP, at early time point of cobalt exposure. Both P2X and P2Y receptors have been shown to be involved in the $[Ca^{2+}]_i$ rise caused by ATP in primary cultures of rat astrocytes [76]. Based on the capability of cobalt to bind and modulate P2X receptors [77] it is likely that the inhibition of the response to ATP is due to reduced Ca^{2+} influx through P2X ligand-gated calcium channels. Further experiments are needed to clarify the mechanisms responsible for the inhibition of the ATP response by cobalt in glial cells. ATP signaling is a relevant target of toxicity because it is implicated in cell-to-cell communication in the brain. Stimulation of astrocytes with ATP causes a propagating wave of $[Ca^{2+}]_i$ rise that regulates communication with other astrocytes as well as with other neural cells [76].

It is commonly accepted that astrocytes are less susceptible than neurons to hypoxia. This is due, at least in part, to the fact that astrocytes can compensate the lack of oxygen by switching from oxidative phosphorylation to the glycolytic pathway. On the contrary, neurons rely on oxygen for ATP generation and do not increase anaerobic metabolism to maintain energy production upon inhibition of oxidative phosphorylation [78]. However, prolonged hypoxia results also in cytotoxicity in astrocytes [79]. Similarly to oxygen deprivation, cobalt exposure has been shown to cause cellular damage in both neurons and astrocytes. In contrast, there is yet no evidence that the susceptibility to cobalt differ between cell types. Neurons and astrocytes, as well as other type of cells, are affected in the same range of doses [17,19,20,22,80]. Previous work [17,19,22,80] and the present study point to common toxicity mechanism. These include increased generation of ROS and mitochondrial damage with release of mitochondrial factors that lead to apoptosis [17,19,22,80]. Another feature reported to occur in both types of neural cells is an increased expression of MAP kinases, which are well known for their cell proliferation and differentiation-inducing pathways and are also associated with apoptosis. In both PC12 neuronal and C6 glioma cell models MAP kinase inhibitors were shown to have protective effects [17,22]. We have also observed increased phosphorylation of both ERK1/2 and p38 in primary astrocytes undergoing cell death (see Supplemental material, Fig. S1) but MAP kinase inhibitors did not reduce cytotoxicity (see Supplemental material, Table S1 and S2), suggesting that the apoptotic pathways induced by cobalt may not be strongly associated with signal transduction via MAP kinases in this type of cells.

In conclusion, we provide novel evidence that cobalt causes numerous toxic effects in primary glial cells. These include mitochondrial damage with release of apoptogenic factors, ultimately resulting in cell death by apoptosis. Several molecular pathways stimulated by cobalt, e.g. the expression of HIF-1α regulated genes and the mode of cell death, are reminiscent of events caused by oxygen deprivation in brain cells, but cobalt seems to have also specific intracellular targets. The characterized end-points of toxicity will be useful in future studies aiming to identify responses of astrocytes to cobalt in vivo and provide a platform for using cobalt as a mimic of hypoxia in glial cells.

Acknowledgments

The authors are grateful to Dr. Ping Sheng Hu for valuable help with the intracellular calcium measurements. This work was supported by Karolinska Institutet, the Swedish Science Research Council (2553), European Commission (LSHM-CT-

2005-518189), the Swedish Brain Foundation, the T. Nilson Foundation, the Swedish Society of Medicine, the Å. Wiberg Foundation and the General Maternity Hospital foundation. The funding agencies do not take any responsibility for the contents of the article.

Appendix A. Supplementary data

Supplementary data associated with this article can be found, in the online version, at doi:10.1016/j.bcp.2006.11.008.

REFERENCES

[1] Elinder C, Friberg L. Cobalt. In: Friberg L, Nordberg G, Voulk V, editors. Handbook on the toxicology of metals. Amsterdam: Elsevier; 1986. p. 211–32.
[2] Stabler SP, Allen RH. Vitamin B12 deficiency as a worldwide problem. Annu Rev Nutr 2004;24:299–326.
[3] Jensen AA, Tuchsen F. Cobalt exposure and cancer risk. Crit Rev Toxicol 1990;20:427–37.
[4] Barceloux DG. Cobalt. J Toxicol Clin Toxicol 1999;37:201–6.
[5] Palmen N. Cobalt and cobalt compounds. Criteria document for Swedish occupational standards. In: Marklund S, editor. Arbete och Hälsa. Stockholm: Arbetslivsinstitutet; 2005.
[6] Ichikawa Y, Kusaka Y, Goto S. Biological monitoring of cobalt exposure, based on cobalt concentrations in blood and urine. Int Arch Occup Environ Health 1985;55:269–76.
[7] Kesteloot H, Roelandt J, Willems J, Claes JH, Joossens JV. An enquiry into the role of cobalt in the heart disease of chronic beer drinkers. Circulation 1968;37: 854–64.
[8] Wehner AP, Busch RH, Olson RJ, Craig DK. Chronic inhalation of cobalt oxide and cigarette smoke by hamsters. Am Ind Hyg Assoc J 1977;38:338–46.
[9] Heath JC. The production of malignant tumours by cobalt in the rat. Br J Cancer 1956;10:668–73.
[10] Jordan CM, Whitman RD, Harbut M. Memory deficits and industrial toxicant exposure: a comparative study of hard metal, solvent and asbestos workers. Int J Neurosci 1997;90:113–28.
[11] Persson E, Henriksson J, Tjalve H. Uptake of cobalt from the nasal mucosa into the brain via olfactory pathways in rats. Toxicol Lett 2003;145:19–27.
[12] Czarnota M, Whitman D, Berman R. Activity and passive-avoidance learning in cobalt-injected rats. Int J Neurosci 1998;93:29–33.
[13] Hasan M, Ali S, Anwar J. Cobalt-induced depletion of dopamine, norepinephrine & 5-hydroxytryptamine concentration in different regions of the rat brain. Indian J Exp Biol 1980;18:1051–3.
[14] Gerber U, Gahwiler BH. Cobalt blocks postsynaptic responses induced by neurotransmitters in the hippocampus in vitro. Neurosci Lett 1991;134:53–6.
[15] Wang G, Hazra TK, Mitra S, Lee HM, Englander EW. Mitochondrial DNA damage and a hypoxic response are induced by CoCl(2) in rat neuronal PC12 cells. Nucleic Acids Res 2000;28:2135–40.
[16] Olivieri G, Hess C, Savaskan E, Ly C, Meier F, Baysang G, et al. Melatonin protects SHSY5Y neuroblastoma cells from cobalt-induced oxidative stress, neurotoxicity and increased beta-amyloid secretion. J Pineal Res 2001;31:320–5.
[17] Yang SJ, Pyen J, Lee I, Lee H, Kim Y, Kim T. Cobalt chloride-induced apoptosis and extracellular signal-regulated protein kinase 1/2 activation in rat C6 glioma cells. J Biochem Mol Biol 2004;37:480–6.
[18] Huk OL, Catelas I, Mwale F, Antoniou J, Zukor DJ, Petit A. Induction of apoptosis and necrosis by metal ions in vitro. J Arthroplasty 2004;19:84–7.
[19] Zou W, Yan M, Xu W, Huo H, Sun L, Zheng Z, et al. Cobalt chloride induces PC12 cells apoptosis through reactive oxygen species and accompanied by AP-1 activation. J Neurosci Res 2001;64:646–53.
[20] Araya J, Maruyama M, Inoue A, Fujita T, Kawahara J, Sassa K, et al. Inhibition of proteasome activity is involved in cobalt-induced apoptosis of human alveolar macrophages. Am J Physiol Lung Cell Mol Physiol 2002;283:L849–58.
[21] Graham RM, Frazier DP, Thompson JW, Haliko S, Li H, Wasserlauf BJ, et al. A unique pathway of cardiac myocyte death caused by hypoxia-acidosis. J Exp Biol 2004;207:3189–200.
[22] Zou W, Zeng J, Zhuo M, Xu W, Sun L, Wang J, et al. Involvement of caspase-3 and p38 mitogen-activated protein kinase in cobalt chloride-induced apoptosis in PC12 cells. J Neurosci Res 2002;67:837–43.
[23] Chandel NS, Vander Heiden MG, Thompson CB, Schumacker PT. Redox regulation of p53 during hypoxia. Oncogene 2000;19:3840–8.
[24] Jones NM, Bergeron M. Hypoxic preconditioning induces changes in HIF-1 target genes in neonatal rat brain. J Cereb Blood Flow Metab 2001;21:1105–14.
[25] Epstein AC, Gleadle JM, McNeill LA, Hewitson KS, O'Rourke J, Mole DR, et al. *C. elegans* EGL-9 and mammalian homologs define a family of dioxygenases that regulate HIF by prolyl hydroxylation. Cell 2001;107:43–54.
[26] Wiesener MS, Maxwell PH. HIF and oxygen sensing; as important to life as the air we breathe? Ann Med 2003;35:183–90.
[27] Sharp FR, Bernaudin M. HIF1 and oxygen sensing in the brain. Nat Rev Neurosci 2004;5:437–48.
[28] Bruick RK. Expression of the gene encoding the proapoptotic Nip3 protein is induced by hypoxia. Proc Natl Acad Sci USA 2000;97:9082–7.
[29] Aschner M. Astrocytic functions and physiological reactions to injury: the potential to induce and/or exacerbate neuronal dysfunction—a forum position paper. Neurotoxicology 1998;19:7–17.
[30] Volterra A, Meldolesi J. Astrocytes, from brain glue to communication elements: the revolution continues. Nat Rev Neurosci 2005;6:626–40.
[31] Yu AC, Wong HK, Yung HW, Lau LT. Ischemia-induced apoptosis in primary cultures of astrocytes. Glia 2001;35:121–30.
[32] Benjelloun N, Joly LM, Palmier B, Plotkine M, Charriaut-Marlangue C. Apoptotic mitochondrial pathway in neurones and astrocytes after neonatal hypoxia-ischaemia in the rat brain. Neuropathol Appl Neurobiol 2003;29:350–60.
[33] Giffard RG, Swanson RA. Ischemia-induced programmed cell death in astrocytes. Glia 2005;50:299–306.
[34] Daré E, Li W, Zhivotovsky B, Yuan X, Ceccatelli S. Methylmercury and H_2O_2 provoke lysosomal damage in human astrocytoma D384 cells followed by apoptosis. Free Radic Biol Med 2001;30:1347–56.
[35] Yee S, Choi BH. Oxidative stress in neurotoxic effects of methylmercury poisoning. Neurotoxicology 1996;17:17–26.
[36] Merker K, Hapke D, Reckzeh K, Schmidt H, Lochs H, Grune T. Copper related toxic effects on cellular protein metabolism in human astrocytes. Biofactors 2005;24: 255–61.

[37] Im JY, Paik SG, Han PL. Cadmium-induced astroglial death proceeds via glutathione depletion. J Neurosci Res 2006;83:301–8.
[38] Hazell AS. Astrocytes and manganese neurotoxicity. Neurochem Int 2002;41:271–7.
[39] Winkler DG, Park I, Kim T, Payne NS, Walsh CT, Strominger JL, et al. Phosphorylation of Ser-42 and Ser-59 in the N-terminal region of the tyrosine kinase p56lck. Proc Natl Acad Sci USA 1993;90:5176–80.
[40] Daré E, Tofighi R, Nutt L, Vettori MV, Emgård M, Mutti A, et al. Styrene 7,8-oxide induces mitochondrial damage and oxidative stress in neurons. Toxicology 2004;201:125–32.
[41] Daré E, Tofighi R, Vettori MV, Momoi T, Poli D, Saido TC, et al. Styrene 7,8-oxide induces caspase activation and regular DNA fragmentation in neuronal cells. Brain Res 2002;933:12–22.
[42] Vanden Hoek TL, Li C, Shao Z, Schumacker PT, Becker LB. Significant levels of oxidants are generated by isolated cardiomyocytes during ischemia prior to reperfusion. J Mol Cell Cardiol 1997;29:2571–83.
[43] Heid CA, Stevens J, Livak KJ, Williams PM. Real time quantitative PCR. Genome Res 1996;6:986–94.
[44] Chunn JL, Young HW, Banerjee SK, Colasurdo GN, Blackburn MR. Adenosine-dependent airway inflammation and hyperresponsiveness in partially adenosine deaminase-deficient mice. J Immunol 2001;167:4676–85.
[45] Ehrenberg B, Montana V, Wei MD, Wuskell JP, Loew LM. Membrane potential can be determined in individual cells from the nernstian distribution of cationic dyes. Biophys J 1988;53:785–94.
[46] Gupta S. Molecular steps of death receptor and mitochondrial pathways of apoptosis. Life Sci 2001;69: 2957–64.
[47] Gabai VL, Meriin AB, Yaglom JA, Volloch VZ, Sherman MY. Role of Hsp70 in regulation of stress-kinase JNK: implications in apoptosis and aging. FEBS Lett 1998;438:1–4.
[48] Pourahmad J, O'Brien PJ, Jokar F, Daraei B. Carcinogenic metal induced sites of reactive oxygen species formation in hepatocytes. Toxicol In Vitro 2003;17:803–10.
[49] Deneke SM. Thiol-based antioxidants. Curr Top Cell Regul 2000;36:151–80.
[50] Aruoma OI, Halliwell B, Hoey BM, Butler J. The antioxidant action of N-acetylcysteine: its reaction with hydrogen peroxide, hydroxyl radical, superoxide, and hypochlorous acid. Free Radic Biol Med 1989;6:593–7.
[51] Wu TW, Fung KP, Zeng LH, Wu J, Nakamura H. Propyl gallate as a hepatoprotector in vitro and in vivo. Biochem Pharmacol 1994;48:419–22.
[52] Mooradian AD. Antioxidant properties of steroids. J Steroid Biochem Mol Biol 1993;45:509–11.
[53] Vengellur A, LaPres JJ. The role of hypoxia inducible factor 1alpha in cobalt chloride induced cell death in mouse embryonic fibroblasts. Toxicol Sci 2004;82:638–46.
[54] Vande Velde C, Cizeau J, Dubik D, Alimonti J, Brown T, Israels S, et al. BNIP3 and genetic control of necrosis-like cell death through the mitochondrial permeability transition pore. Mol Cell Biol 2000;20:5454–68.
[55] Nordlind K. Expression of heat shock proteins in heavy metal-provoked inflamed human skin. Immunopharmacol Immunotoxicol 2002;24:383–94.
[56] Holm RH, Kennepohl P, Solomon EI. Structural and functional aspects of metal sites in biology. Chem Rev 1996;96:2239–314.
[57] Maines MD. Heme oxygenase: function, multiplicity, regulatory mechanisms, and clinical applications. Fed Am Soc Exp Biol J 1988;2:2557–68.
[58] Wiberg GS. The effect of cobalt ions on energy metabolism in the rat. Can J Biochem 1968;46:549–54.
[59] Clyne N, Hofman-Bang C, Haga Y, Hatori N, Marklund SL, Pehrsson SK, et al. Chronic cobalt exposure affects antioxidants and ATP production in rat myocardium. Scand J Clin Lab Invest 2001;61:609–14.
[60] Hatori N, Pehrsson SK, Clyne N, Hansson G, Hofman-Bang C, Marklund SL, et al. Acute cobalt exposure and oxygen radical scavengers in the rat myocardium. Biochim Biophys Acta 1993;1181:257–60.
[61] Joza N, Susin SA, Daugas E, Stanford WL, Cho SK, Li CY, et al. Essential role of the mitochondrial apoptosis-inducing factor in programmed cell death. Nature 2001;410:549–54.
[62] Grasselli F, Basini G, Bussolati S, Bianco F. Cobalt chloride, a hypoxia-mimicking agent, modulates redox status and functional parameters of cultured swine granulosa cells. Reprod Fertil Dev 2005;17:715–20.
[63] Chandel NS, Maltepe E, Goldwasser E, Mathieu CE, Simon MC, Schumacker PT. Mitochondrial reactive oxygen species trigger hypoxia-induced transcription. Proc Natl Acad Sci USA 1998;95:11715–20.
[64] Kadiiska MB, Maples KR, Mason RP. A comparison of cobalt(II) and iron(II) hydroxyl and superoxide free radical formation. Arch Biochem Biophys 1989;275:98–111.
[65] Tomaro ML, Frydman J, Frydman RB. Heme oxygenase induction by $CoCl_2$, Co-protoporphyrin IX, phenylhydrazine, and diamide: evidence for oxidative stress involvement. Arch Biochem Biophys 1991;286:610–7.
[66] BelAiba RS, Djordjevic T, Bonello S, Flugel D, Hess J, Kietzmann T, et al. Redox-sensitive regulation of the HIF pathway under non-hypoxic conditions in pulmonary artery smooth muscle cells. Biol Chem 2004;385:249–57.
[67] Tan S, Sagara Y, Liu Y, Maher P, Schubert D. The regulation of reactive oxygen species production during programmed cell death. J Cell Biol 1998;141:1423–32.
[68] Aley PK, Murray HJ, Boyle JP, Pearson HA, Peers C. Hypoxia stimulates Ca^{2+} release from intracellular stores in astrocytes via cyclic ADP ribose-mediated activation of ryanodine receptors. Cell Calcium 2006;39:95–100.
[69] Kiss T, Osipenko ON. Toxic effects of heavy metals on ionic channels. Pharmacol Rev 1994;46:245–67.
[70] Hasselblatt M, Paulus W. Astrocytic gene expression profiling upon hypoxia. Neuroreport 2006;17:51–4.
[71] Wiener CM, Booth G, Semenza GL. In vivo expression of mRNAs encoding hypoxia-inducible factor 1. Biochem Biophys Res Commun 1996;225:485–8.
[72] Yu R, Gao L, Jiang S, Guan P, Mao B. Association of HIF-1alpha expression and cell apoptosis after traumatic brain injury in the rat. Chin J Traumatol 2001;4:218–21.
[73] Yamaura K, Gebremedhin D, Zhang C, Narayanan J, Hoefert K, Jacobs ER, et al. Contribution of epoxyeicosatrienoic acids to the hypoxia-induced activation of Ca(2+)-activated K(+) channel current in cultured rat hippocampal astrocytes. Neuroscience 2006;143:703–16.
[74] Vengellur A, Woods BG, Ryan HE, Johnson RS, LaPres JJ. Gene expression profiling of the hypoxia signaling pathway in hypoxia-inducible factor 1alpha null mouse embryonic fibroblasts. Gene Exp 2003;11:181–97.
[75] MacVicar BA. Morphological differentiation of cultured astrocytes is blocked by cadmium or cobalt. Brain Res 1987;420:175–7.
[76] Abbracchio MP, Verderio C. Pathophysiological roles of P2 receptors in glial cells. Novartis Found Symp 2006;276:91–103 (discussion 12, 275–81).
[77] Coddou C, Lorca RA, Acuna-Castillo C, Grauso M, Rassendren F, Huidobro-Toro JP. Heavy metals modulate the activity of the purinergic P2X4 receptor. Toxicol Appl Pharmacol 2005;202:121–31.
[78] Almeida A, Almeida J, Bolanos JP, Moncada S. Different responses of astrocytes and neurons to nitric oxide: the

role of glycolytically generated ATP in astrocyte protection. Proc Natl Acad Sci USA 2001;98:15294–9.
[79] Horvat S, Beyer C, Arnold S. Effect of hypoxia on the transcription pattern of subunit isoforms and the kinetics of cytochrome c oxidase in cortical astrocytes and cerebellar neurons. J Neurochem 2006;99:937–51.
[80] Kotake-Nara E, Takizawa S, Quan J, Wang H, Saida K. Cobalt chloride induces neurite outgrowth in rat pheochromocytoma PC-12 cells through regulation of endothelin-2/vasoactive intestinal contractor. J Neurosci Res 2005;81:563–71.